Zhi-Qiang Du ORCID iD: 0000-0002-6758-3023

Xu Fang ORCID iD: 0000-0002-7638-1116

Rewiring central carbon metabolism for tyrosol and salidroside production in *Saccharomyces cerevisiae*

Authors

Wei Guo[1], Qiulan Huang[1], Yuhui Feng[1], Taicong Tan[1], Suhao Niu[1], Shaoli Hou[2], Zhigang Chen[1], Zhi-Qiang Du[1*], Yu Shen[1*], Xu Fang[1, 3*]

Affiliations

[1] State Key Laboratory of Microbial Technology, Shandong University, Qingdao 266237, China

[2] Yantai Huakangrongzan Biotechnology Co., Ltd, Yantai 264006, China

[3] National Glycoengineering Research Center, Shandong University, Qingdao 266237, China

***Correspondence:**

Xu Fang (E-mail: fangxu@sdu.edu.cn); Yu Shen (E-mail: shenyu@sdu.edu.cn); Zhi-Qiang Du (E-mail: zhiqiangdu@sdu.edu.cn); Addresses: No. 72, Binhai Road, Jimo District, Qingdao, Shandong Province, China.

This article has been accepted for publication and undergone full peer review but has not been through the copyediting, typesetting, pagination and proofreading process, which may lead to differences between this version and the Version of Record. Please cite this article as doi: 10.1002/bit.27370.

Fundings:

The National Key R&D Program of China (No. 2018YFA090010), Major Program of Shandong Province Natural Science Foundation (No. ZR2018ZB0209), Key Technologies R&D Program of Shandong Province (No. 2018GSF121021), the 111 Project (No. B16030), the State Key Laboratory of Microbial Technology Open Projects Fund and National Natural Science Foundation of China (Nos.31570040 and 31870785).

Running title：Metabolic engineering for tyrosol production

Abstract

Metabolic engineering of *Saccharomyces cerevisiae* for high level production of aromatic chemicals has received increasing attention in recent years. Tyrosol production from glucose by *S. cerevisiae* is considered an environmentally sustainable and safe approach. However, the production of tyrosol and salidroside by engineered *S. cerevisiae* has been reported to be lower than 2 g/L to date. In this study, *S. cerevisiae* was engineered with a push-pull-restrain strategy to efficiently produce tyrosol and salidroside from glucose. The biosynthetic pathways of ethanol, phenylalanine and tryptophan were restrained by disrupting *PDC1*, *PHA2* and *TRP3*. Subsequently, tyrosol biosynthesis was enhanced with a metabolic pull strategy of introducing *PcAAS* and $EcTyrA^{M53I/A354V}$. Moreover, a metabolic push strategy was implemented with the heterologous expression of phosphoketolase (Xfpk), and then Erythrose 4-phosphate was synthesized simultaneously by two pathways, the Xfpk-based pathway and the pentose phosphate pathway, in *S. cerevisiae*. Furthermore, the heterologous expression of Xfpk alone in *S. cerevisiae* efficiently improved tyrosol production compared with

the coexpression of Xfpk and phosphotransacetylase. Finally, the tyrosol yield increased by approximately 135-folds, compared with that of parent strain. The total amount of tyrosol and salidroside with glucose fed-batch fermentation was over 10 g/L and reached levels suitable for large-scale production.

Keywords: $_{D}$-erythrose 4-phosphate, *Saccharomyces cerevisiae,* salidroside, phosphoketolase, tyrosol.

Introduction

Tyrosol, which mainly exists in olive oil, wine, and plant tissues, is a phenethyl alcohol derivative known to possess antioxidant and anti-inflammatory effects (Choe et al., 2012). Tyrosol is the precursor of salidroside and hydroxytyrosol, which are important cardiovascular drugs widely used in the pharmaceutical industry (Granados-Principal et al., 2010; Zhu et al., 2015; Chung et al., 2017). The biosynthesis of tyrosol and salidroside from sugars has attracted increasing attention because of certain advantages, such as being environmentally friendly, requiring low energy consumption, and having effective production methods and simplicity of operation. Therefore, technologies exploiting biosynthetic pathways in microorganisms for tyrosol production should be developed.

Saccharomyces cerevisiae has been widely used as a microbial cell factory in industrial biotechnology due to its safety, high fermentation efficiency, and robustness to harsh fermentation conditions (Nielsen, 2019). Tyrosol has been natively biosynthesized in *S. cerevisiae* via the Ehrlich pathway (Hazelwood et al., 2008). In recent years, scientists have attempted to modify the tyrosol biosynthesis pathway in *S. cerevisiae* to improve the tyrosol yield (Jiang et al., 2018; Guo et al., 2019). However, the production of tyrosol in *S. cerevisiae* has been reported to

be lower than 2 g/L to date. The large-scale production of tyrosol in *S. cerevisiae* is difficult to achieve based on such a low yield of tyrosol.

In *S. cerevisiae*, the shikimate pathway is an indispensable pathway for the biosynthesis of aromatic derivatives and provides the main carbon skeleton for the biosynthesis of aromatic compounds (Lee and Wendisch, 2017). Phosphoenolpyruvate (PEP) and $_D$-erythrose 4-phosphate (E4P) are the precursors of the shikimate pathway and are condensed into 3-deoxy-$_D$-arabinoheptulosonate 7-phosphate (DAHP) under the catalytic action of 3-deoxy-$_D$-arabinoheptulosonate 7-phosphate synthases (Aro3p andAro4p), which is the initiating and rate-limiting step of the shikimate pathway (Averesch and Kromer, 2018). Improvements in the availability of PEP and E4P have been suggested to be the key to increasing the carbon flux of the shikimate pathway (Bilal et al., 2018).

In *S. cerevisiae*, PEP is a key intermediate metabolite in the glycolytic pathway. Most PEP in *S. cerevisiae* is converted to pyruvate (PYR) under the catalytic action of pyruvate kinase (Pyk1p and Pyk2p), and less than 8% PEP enters the shikimate pathway (Suastegui et al., 2016). Researchers who attempted to reduce the flux toward pyruvate by engineering pyruvate kinases found that reducing the activity of pyruvate kinase results in the accumulation of PEP, however, it does not increase the flux into the shikimate pathway, resulting in growth defects when glucose is the only carbon source (Gruning et al., 2011; Gold et al., 2015). In addition, approaches designed to reduce the activity of pyruvate decarboxylases (Pdcp) have been introduced to reduce the flux from PYR toward the production of ethanol during the fermentation of *S. cerevisiae*. The disruption

of *PDC1* in *S. cerevisiae* has been shown to reduce the activity of pyruvate decarboxylases by approximately 30% (Wang et al., 2015). As shown in our previous study, the deletion of *PDC1* in *S. cerevisiae* improves tyrosol production by 32.49% (Guo et al., 2019).

Apart from the availability of the precursor PEP, an imbalance in the amount of the precursors PEP and E4P derived from the pentose phosphate pathway (PP pathway) is a major problem impeding the production of aromatic amino compounds. In *S. cerevisiae*, glucose-6-phosphate dehydrogenase (Zwf1p) catalyzes the entry and rate-limiting step of the PP pathway by converting $_{D}$-glucose 6-phosphate (G6P) from glucose into 6-phospho $_{D}$-glucono-1,5-lactone (6PGL) (Minard and McAlister-Henn, 2005). Subsequently, 6PGL is converted into $_{D}$-erythrose 4-phosphate (E4P) through several steps. Overexpression of *ZWF1* in *Pichia pastoris* has been shown to result in a 6% increase in the carbon flux of the PP pathway (Nocon et al., 2016).

In addition to the PP pathway, the phosphoketolase (PHK) pathway includes phosphoketolase (EC 4.1.2.22, Xfpk) and phosphotransacetylase (EC 2.3.1.8, Pta) (Bergman et al., 2016). Xfpk could convert $_{D}$-fructose 6-phosphate (F6P) or $_{D}$-xylulose 5-phosphate (X5P) into the corresponding aldose phosphate (E4P or $_{D}$-glyceraldehyde 3-phosphate (GAP), respectively) and generate one molecule of acetyl phosphate (AcP); AcP is then reversibly converted into acetyl-CoA by Pta (Castaño-Cerezo et al., 2009).

In this study, we aimed to efficiently biosynthesize tyrosol and salidroside from glucose with a push-pull-restrain strategy for modifying three modules in *S. cerevisiae* (Fig. 1). In the blue module, the biosynthetic pathways of ethanol,

phenylalanine and tryptophan were restrained by disrupting *PDC1*, *PHA2* and *TRP3*. In the orange module, tyrosol biosynthesis was enhanced by the introduction of *PcAAS* and *EcTyrA*$^{M53I/A354V}$ as metabolic pull signals. In the yellow and green module, a metabolic push strategy was implemented by introducing the Xfpk-based pathway, and then E4P was synthesized simultaneously via two pathways, the Xfpk-based pathway and the PP pathway, in *S. cerevisiae*. The final tyrosol and salidroside titers reached 8.48 g/L and 1.82 g/L via fed-batch fermentation, which are the maximum total titer of tyrosol and salidroside reported to date, whether in *S. cerevisiae* or *E. coli*. This metabolic engineering strategy can be further extended to facilitate the large-scale production of other aromatic amino acid derivatives.

Materials and Methods

Strains and culture conditions

The industrial *S. cerevisiae* strain HLF-Dα was used as an original strain in this study. The *E. coli* strain GB05-dir was used to construct the recombinant plasmids via homologous recombineering method (Fu et al., 2012). The following antibiotics were used for selection: 500 μg/mL geneticin sulfate; hygromycin B, 250 μg/mL; nourseothricin, 200 μg/mL; ampicillin, 100 μg/mL and tetracycline, 4 μg/mL. Geneticin sulfate, ampicillin, and tetracycline were purchased from Genview (Beijing, China), hygromycin B was purchased from Amresco (Solon, USA), nourseothricin sulfate was purchased from Werner BioAgents (Jena, Germany), and yeast extract and tryptone were purchased from Oxoid (Basingstoke, England). Other chemicals, if not specified otherwise, were purchased from Sinopharm Chemical Reagent Co, Ltd (Shanghai, China).

All the shake flasks fermentation was performed in 300 mL shake flasks containing 50 mL of YPD liquid medium (Containing 10 g/L yeast extract, 20 g/L tryptone, and 20 g/L glucose) at 30 °C with constant orbital shaking at 250 rpm, if not specified otherwise. The pulse fed-batch fermentation was conducted in shake flasks, followed by the addition of 20 g/L glucose at 24 and 48 h. The glucose fed-batch fermentation was performed in a 3 L fermenter (Winpact, USA) containing 1.5 L of YPD liquid medium, at 300 rpm, with an airflow rate of 1 vvm, and at a temperature of 30 °C and a pH of 6.5 ± 0.5. Glucose was added to the fermenter at a rate of 1.6 g/L/h after glucose supplementation was initiated at 11.5 h. The shake-flask fermentation experiments were performed in triplicate, and data are presented as means ± standard errors (s.e.m). The fed-batch fermentation was conducted twice.

Construction of plasmids, linearized expression cassettes, and strains

All the plasmids and cassettes constructed and used in this study are listed in Table S1. Strains constructed and used in this study are listed in Table 3. The plasmid pAG32 (Goldstein and McCuske, 1999) and *natMX* (Sadowski et al., 2008) were supplied by Professor Xiaoming Bao and Professor Liangran Zhang, respectively. The genes encoding phosphoketolases from *Bifidobacterium adolescentis* (*Baxfpk*, GenBank: BAF39468.1), *Bifidobacterium breve* (*Bbxfpk*, GenBank: KND53308.1), and *Bifidobacterium dentium* (*Bdxfpk*, GenBank: BAQ26957.1), phosphotransacetylase from *Clostridium kluyveri* (*Ckpta*, GenBank: WP_012101779.1), tyrosine decarboxylase from *Petroselinum crispum* (*PcAAS*, GenBank: AAA33860.1), and UDP-glycosyltransferase from *Arabidopsis thaliana* (*ugt85a1*, GenBank: NP_173656.1) were codon-optimized

and synthesized by BGI (Beijing, China) for *S. cerevisiae*. The plasmids and cassettes were constructed as previously reported (Jiang et al., 2020). All the promoters and terminators were amplified using the genome of *S. cerevisiae* HLF-Dα as the template. All the primers are listed in Table S2. Molecular genetic operations of *E. coli* and *S. cerevisiae* were performed as described in our previous study (Guo et al., 2019). All the gene disruptions and genomic integrations were verified by PCR amplification and sequencing. The Cre–loxP recombination system established based on the plasmids pCH and pUG6 was applied to remove the selectable marker from industrial *S. cerevisiae* strains using the approach reported by Gueldener et al. (2002).

Measurement of the biomass

The absorbance of the broth was measured as previously described (Guo et al., 2019). The biomass was defined as grams of dry cell weight per liter and correlated to the dry cell weight (DCW) with DCW/optical density (OD) = 0.3969.

Analysis of metabolites using HPLC

All the metabolites were analyzed with the Elite LaChrom HPLC system (HITACHI, Japan). Glucose, ethanol, and acetate concentrations in the supernatant of the centrifuged fermentation broth were analyzed as previously described (Wang et al., 2016). The tyrosol and salidroside concentrations were detected with a diode array detector and a C18 reverse-phase chromatography column (Imtakt C18 column, 150 × 4.6 mm, 3 μm), and the HPLC conditions were consistent with our previous study (Guo et al., 2019).

Measurements of glucose-6-phosphate dehydrogenase activity and phosphoketolase activity

The glucose-6-phosphate dehydrogenase (Zwf1p) activity assay was based on the measurements of NADPH production. The analytical method was conducted using the method reported by Plomer and Gafni (1992). Phosphoketolase activity was analyzed using the method reported by Bergman et al. (2016). All chemicals used in the enzyme activity assays were purchased from Aladdin Ltd (Shanghai, China), unless specified otherwise. Specific activity of Zwf1p was normalized to the amount of protein used in the assay (U/mg total protein) and calculated with a millimolar extinction coefficient of 6.22 for NADPH. The units of the specific activity of Xfpk were defined as the amount of the product AcP (μmol/L) produced per minute per milligram of total protein at 37 ℃, and the enzyme activity was defined as the total amount of protein (mg) required to generate 1 μmol of AcP per minute. All the enzyme activity assays were performed in triplicate, and data are presented as the means ± s.e.m.

Results and discussions

Screening and constructing an efficient tyrosol-producing platform in *S. cerevisiae*

In *S. cerevisiae*, tyrosol is an aromatic fusel biosynthesized by the Ehrlich pathway following the shikimate pathway. According to Suastegui et al. (2016), the metabolic flux of the natural shikimate pathway varies among different *S. cerevisiae* strains owing to the different flux distributions at some key nodes related to the biosynthetic pathways of aromatic compounds. Therefore, it is necessary to screen a suitable industrial host for tyrosol production. A haploid

industrial *S. cerevisiae* strain HLF-Dα was isolated from *S. cerevisiae* industrial strains preserved in our lab for tyrosol biosynthesis. The tyrosol titer of HLF-Dα strain reached 62.16 mg/L after 60 h of shake-flask cultivation, which was higher than those of other strains. Therefore, the industrial strain HLF-Dα was used as the original strain for constructing a tyrosol-producing platform in this study.

As shown in our previous study, the construction of a new connection between tyrosine and tyrosol and engineering the chorismate-related pathway leads to a significant increase in tyrosol production in *S. cerevisiae* (Guo et al., 2019). Moreover, tyrosol production is improved with disruption of *PDC1* in *S. cerevisiae* without significant effect on cell growth and ethanol production (Guo et al., 2019). Therefore, similar strategies of deleting *PDC1* and overexpressing $EcTyrA^{M53I/A354V}$ and *PcAAS* were employed in the HLF-Dα strain to construct strain DA-1. The tyrosol concentration produced by strain DA-1 was 742.02 ± 22.45 mg/L and was 11-fold higher than the parent strain HLF-Dα after 72 h of shake-flask cultivation. *S. cerevisiae* strain DA-1 was used as the tyrosol-producing platform strain for further metabolic engineering in this study.

Pulse fed-batch fermentation in shake flasks was performed to investigate the distribution of carbon flux between the central carbon metabolism and tyrosol biosynthesis pathway. Twenty grams of glucose per liter were fed into the flasks when the strain DA-1 was cultured for 24 and 48 h. Feeding glucose with pulse fed-batch fermentation did not alter the tyrosol concentration (Fig. S1B), though substantial differences in the biomass and ethanol production were observed between the batch and pulse fed-batch fermentations (Fig. S1C and S1D). Thus, we speculated that although the biosynthesis of the PEP intermediate in glycolysis

was enhanced by feeding glucose, the lack of an increase in tyrosol production might be attributed to the lack of E4P supplied by the PP pathway, resulting in an imbalance of the precursors PEP and E4P required for tyrosol biosynthesis.

Enhancing the PP pathway by overexpressing *ZWF1* did not increase tyrosol production

Aromatic compounds are almost exclusively synthesized through the shikimate pathway, and the amount of DAHP formed as the precursor is the rate-limiting step of the shikimate pathway (Averesch and Kromer, 2018). Meanwhile, the synthesis of DAHP is restricted by the limited amount of E4P produced via the PP pathway in *S. cerevisiae* (Gottardi et al., 2017). Based on the results shown in Fig. S1, we speculated that the lack of E4P produced by the PP pathway limited tyrosol production. Therefore, we attempted to enhance the first and rate-limiting step of the PP pathway that catalyzes G6P into 6PGL by glucose-6-phosphate dehydrogenase (Zwf1p). *ZWF1* was overexpressed in the locus of *PHA2* in the strain DA-1, resulting in the strain DA-3. As shown in Fig. S2A, the Zwf1p activity (13.99 ± 0.15 U/mg total protein) increased by 284.49% after overexpressing *ZWF1*. It was reported that the overexpression of *ZWF1* contributes to an increase in the flux from glycolysis to the PP pathway and produces more NADPH for cell growth and energy metabolism (Nocon et al., 2016). However, no obvious increase in cell growth or tyrosol production was observed in *ZWF1* overexpressed strain DA-3 compared with that in DA-1 and DA-2 at 48 and 72 h cultivation, although the tyrosol production of DA-3 was higher than that of DA-2 and DA-1 at 24 h (Fig. 2). We speculated that the carbon flux towards the PP pathway was somewhat increased owe to the overexpression

of *ZWF1* in strain DA-3, as the tyrosol production was enhanced to a certain extend before 24 h. After glucose was depleted, intermediates accumulated in the PP pathway might be used for cell growth so that there was no significant change in cell growth or tyrosol production by DA-1, DA-2 and DA-3 at 48 or 72 h cultivation.

Pathway thermodynamics identified the Xfpk-based pathway as the preferred pathway for generating E4P

To find a more effective E4P biosynthesis pathway, the Xfpk-based pathway and the PP pathway initiated by Zwf1p-mediated catalysis were compared based on the thermodynamic parameters calculated using eQuilibrator (Flamholz et al., 2012). As shown in Table 1, the predicted thermodynamic data indicated that the total Gibbs energy change ($\Delta_r G'^{m}$) of the Xfpk-based pathway (2 $_D$-glucose + 2 orthophosphate + 2 ATP = 2 $_D$-erythrose 4-phosphate + 2 ADP + 2 acetyl phosphate + 2 H_2O) was −129.2 kJ/mol, which was less than that of the PP pathway (2 $_D$-glucose + 4 $NADP^+$ + 2 ATP + 2 H_2O = $_D$-erythrose 4-phosphate + 4 NADPH + 4 H^+ + 2 ADP + 2 CO_2 + $_D$-fructose-6-phosphate; $\Delta_r G'^{m}$ = −102.7 kJ/mol). The Max-min Driving Force (MDF) of the Xfpk-based pathway was 20.3 kJ/mol, which was approximately two-fold higher than that of the PP pathway (10.3 kJ/mol). Furthermore, the biosynthesis of E4P from glucose via the Xfpk-based pathway only requires three steps and does not require coenzyme factors. The biosynthesis of E4P from glucose via the PP pathway comprises eight steps, and four $NADP^+$ molecules are required to generate each E4P molecule. The theoretical molar yields of the carbon molecules and that of the Xfpk-based pathway were 66.67% and 100%, respectively, which is two-fold of that of the PP

pathway. Based on predicted pathway thermodynamic data and other relevant parameters listed in Table 1, the Xfpk-based pathway was considered as a more conducive pathway for the precursor E4P supply for the shikimate pathway, which may further facilitate the biosynthesis of aromatic amino acids and the production of tyrosol in *S. cerevisiae*.

Introduction of the Xfpk-based pathway in *S. cerevisiae* to improve the tyrosol yield

According to the predicted thermodynamics results (Table 1), the Xfpk-based pathway was more effective at increasing the E4P supply than the PP pathway due to advantages such as a lower $\Delta_r G'^m$, fewer reaction steps, and its lack of a requirement for cofactors. The heterologous expression of Xfpk from *B. breve* in *S. cerevisiae* results in a 540% increase in E4P production (Bergman et al., 2019). Herein, the Xfpk-based pathway was constructed in *S. cerevisiae* by heterologously expressing a codon-optimized *xfpk* gene from *B. adolescentis* (*Baxfpk*) at the loci of *PHA2*, *GRE3*, or *XKS1* in the DA-1 strain, resulting in the *Baxfpk*-overexpressed strains DA-4, DA-6, and DA-8. In *S. cerevisiae*, *PHA2* in *S. cerevisiae* involved in the phenylalanine biosynthesis pathway (Bross et al. 2011), and *GRE3* and *XKS1* are related to xylose metabolism (Seike et al., 2019). The corresponding genes in DA-1 were deleted, generating the strains DA-2 (*pha2*Δ), DA-5 (*gre3*Δ), and DA-7 (*xks1*Δ) as the control strains. As shown in Fig. S3, by expressing *Baxfpk* in DA-1, 141.02 ± 1.38, 121.50 ± 0.79 and 124.53 ± 4.10 mg/g DCW of tyrosol were obtained in strains DA-4, DA-6 and DA-8, respectively, after 72 h of shake-flask cultivation, which was 48.16%, 18.05% and 24.46% higher than that of the control strains DA-2 (95.18 ± 2.70 mg/g DCW), DA-5

(102.91 ± 0.95 mg/g DCW) and DA-7 (100.06 ± 4.25 mg/g DCW), respectively. Compared with the *GRE3* or *XKS1* locus, heterologous expression of *Baxfpk* at the *PHA2* locus was more appropriate for tyrosol biosynthesis in *S. cerevisiae*. We speculate that the carbon flux in the phenylalanine biosynthesis pathway was reduced, because of the disruption of *PHA2* redirected the flux towards tyrosol biosynthesis. Thus, tyrosol yield by DA-4 was higher than those by DA-6 and DA-8.

Furthermore, the *xfpk* gene from *B. breve* or *B. dentium* was introduced at the *PHA2* locus in strain DA-1, generating the strains DA-9 and DA-10. Based on the results of the Xfpk activity assay, Xfpks were expressed in *S. cerevisiae* (Fig. S2B). After 72 h of shake-flask cultivation, the tyrosol yields of strains DA-4, DA-9, and DA-10 reached 872.01 ± 10.53, 927.68 ± 25.26, and 880.63 ± 4.94 mg/L. The tyrosol yields of strains DA-4, DA-9, and DA-10 increased by 25.43%, 33.44%, and 26.67%, compared with that of strain DA-2 (695.40 ± 2.45 mg/L) (Fig. 3A). Thus, the heterologous expression of *Bb*Xfpk preferentially increased tyrosol biosynthesis over *Ba*Xfpk and *Bd*Xfpk. The actual molar yields of glucose to tyrosol by DA-4, DA-9, and DA-10 reached 1.14, 1.21, and 1.15, respectively, and all were higher than that by strain DA-3 (1.01). These results supported our prediction that the introduction of the Xfpk-based pathway was more conducive than enhancing the PP pathway via overexpressing *ZWF1* for tyrosol production in *S. cerevisiae*.

Acetyl phosphate (AcP) is one of the compounds produced from F6P or X5P with the catalysis of Xfpk; it is converted into acetate by glycerol-1-phosphatases (Gpp1p and Gpp2p) in *S. cerevisiae* (Meadows et al., 2016). AcP is also

reversibly converted into acetyl-CoA by Pta (Castano-Cerezo et al., 2009). The disruption of the main glycerol-1-phosphatase gene *GPP1* and heterologous expression of the codon-optimized Pta gene from *C. kluyveri* (*Ckpta*) were simultaneously performed in strain DA-4 to reduce the accumulation of acetate and direct more carbon flux from the AcP node to acetyl-CoA synthesis for cell growth, generating the strain DA-42 (*GPP1*::*Ckpta*). Simultaneously, *GPP1* was disrupted in strain DA-4 and strain DA-41 (*gpp1*Δ) was obtained. As shown in Fig. S4A, there was no change in tyrosol titer between strains DA-41 and DA-4. However, the tyrosol production in strain DA-42 (702.25 ± 7.55 mg/L) was 20.60% lower than that in DA-41 (844.42 ± 14.85 mg/L) after 96 h shake-flask incubation (Fig. S4A). No significant changes were observed in cell growth in DA-4, DA-41, and DA-42 within 96 h of shake-flask cultivation (Fig. S4B). These results indicated that the simultaneous heterologous expression of Xfpk and Pta in *S. cerevisiae* exerted a negative effect on tyrosol production, which was consistent with the result reported by Hassing et al. (2019), the introduction of the PHK pathway in *S. cerevisiae* with a de novo 2-phenylethanol biosynthetic pathway decrease the production of 2-phenylethanol. Liu et al. (2019) did not observe a significant effect of the insertion of the same PHK pathway into *S. cerevisiae* on *p*-coumaric acid production. Our study confirmed that the introduction of the Xfpk-based pathway is an efficient strategy for increasing tyrosol production in *S. cerevisiae*, guided by the rational analysis of thermodynamics information.

Glucose fed-batch fermentation for higher tyrosol production

Fed-batch fermentation of DA-9 was performed in a 3 L lab-scale bioreactor with glucose feeding to further improve tyrosol production. In the glucose-feeding

phase, no glucose was detected, and the maximum biomass reached 22.78 g/L after 48 h of cultivation (Fig. 4A). The tyrosol titer of DA-9 reached up to 8.37 g/L and remained stable after 192 h of cultivation (Fig. 4C). Therefore, the codon-optimized UDP-glycosyltransferase gene from *Arabidopsis thaliana* (*ugt85a1*) was heterologously expressed at the *TRP3* locus and the strain DA-91 was generated. *TRP3* was the indole-3-glycerol-phosphate synthase gene related to tryptophan biosynthesis in *S. cerevisiae* (Soejima et al., 2012). A *TRP3* disrupted strain named DA-9-1 was constructed as a control strain. No significant difference was observed in tyrosol production of DA-9-1 and DA-9 (Figure S5). The maximum biomass of DA-91 reached 23.24 g/L after 322.2 g/L of the total amount of glucose into a 3L bioreactor was utilized (Fig. 4B). Over 10 g/L of the total amount of tyrosol (8.48 g/L) and salidroside (1.82 g/L) was obtained after 192 h cultivation (Fig. 4D), which was 5-fold higher than the highest titer ever reported in yeast (1.39 g/L tyrosol and 0.73 g/L salidroside) (Jiang et al., 2018) though the total amount of utilized glucose of strain DA-91 was 36.82% lower than the amount reported by Jiang et al (2018) (Table 2). The yields of tyrosol and salidroside of strain DA-91 reached 26.32 and 5.65 mg g^{-1} glucose and were 9.64 and 3.92-fold higher than the yields reported by Jiang et al (2018). These results have made possible the large-scale production of tyrosol and salidroside in *S. cerevisiae*.

Conclusions

With the increasing demand for tyrosol in the food, pharmaceutical, and cosmetic industries, scaling-up the production of tyrosol via green and sustainable technologies characterized by lower costs, high purity and a reliable supply is

urgently required and expected. Our study confirmed that the introduction of the Xfpk-based pathway is an efficient strategy for increasing tyrosol production in *S. cerevisiae*, guided by the rational analysis of thermodynamics information. Furthermore, a total tyrosol and salidroside production exceeding 10 g/L was achieved, which is the highest titer reported to date (Table 2). We are confident that the push-pull-restrain strategy used in this study provides insights into potential improvements in the titers of other aromatic amino acid-derived compounds in *S. cerevisiae*.

Acknowledgments

We would like to thank Prof. Luying Xun from Shandong University for his valuable suggestions. We would like to thank Prof. Liangran Zhang from Shandong University for his assistance with in isolating *S. cerevisiae* strains. We would like to thank Dr. Prof. Xiaoming Bao for providing the plasmid vector pAG32, Prof. Dr. Liangran Zhang for providing the *natMX* resistance gene. We would like to thank Chengjia Zhang and Nannan Dong from State Key Laboratory of Microbial Technology of Shandong University for help and guidance in fed-batch fermentation. This study was supported by grants from the National Key R&D Program of China (No. 2018YFA090010), Major Program of Shandong Province Natural Science Foundation (No. ZR2018ZB0209), Key Technologies R&D Program of Shandong Province (No. 2018GSF121021), the 111 Project (No. B16030), the State Key Laboratory of Microbial Technology Open Projects Fund and National Natural Science Foundation of China (Nos. 31870785 and 31570040).

Author contributions

WG, QH, YF, TT, SN and SH performed experiments. WG, SN, YS, ZC and XF were involved in analysis and interpretation of experimental data. WG, ZD and XF wrote the manuscript. WG, ZD and XF conceived of the study.

Conflict of interest

All the authors declare no competing interests.

References

Averesch, N. J. H., & Krömer, J. O. (2018) Metabolic engineering of the shikimate pathway for production of aromatics and derived compounds-present and future strain construction strategies. *Frontiers in Bioengineering and Biotechnology*. *6*, 32. doi.org/10.3389/fbioe.2018.00032.

Bai, Y. F., Bi, H. P., Zhuang, Y. B., Liu, C., Cai, T., Liu, X. N., Zhang, X. L., Liu, T., & Ma, Y. H. (2014) Production of salidroside in metabolically engineered *Escherichia coli*. *Scientific Reports. 4*, 6640. doi.org/10.1038/srep06640.

Bergman, A., Hellgren, J., Moritz, T., Siewers, V., Nielsen, J., & Chen, Y. (2019) Heterologous phosphoketolase expression redirects flux towards acetate, perturbs sugar phosphate pools and increases respiratory demand in *Saccharomyces cerevisiae*. *Microbial Cell Factories*. *18*, 25. doi.org/10.1186/s12934-019-1072-6.

Bergman, A., Siewers, V., Nielsen, J., & Chen, Y. (2016) Functional expression and evaluation of heterologous phosphoketolases in *Saccharomyces cerevisiae*. *AMB Express*. *6*, 115. doi.org/10.1186/s13568-016-0290-0.

Bilal, M., Wang, S., Iqbal, H. M. N., Zhao, Y., Hu, H., Wang, W., & Zhang, X. (2018) Metabolic engineering strategies for enhanced shikimate biosynthesis: current scenario and future developments. *Applied Microbiology and*

Biotechnology. *102*, 7759-7773. doi.org/10.1007/s00253-018-9222-z.

Bross, C. D., Corea, O. R., Kaldis, A., Menassa, R., Bernards, M. A., & Kohalmi, S. E. (2011) Complementation of the *pha2* yeast mutant suggests functional differences for arogenate dehydratases from *Arabidopsis thaliana*. *Plant Physiology and Biochemistry*. *49*, 882-890. doi.org/10.1016/j.plaphy.2011.02.010.

Castaño-Cerezo, S., Pastor, J. M., Renilla, S., Bernal, V., Iborra, J. L., & Cánovas, M. (2009) An insight into the role of phosphotransacetylase (pta) and the acetate/acetyl-CoA node in *Escherichia coli*. *Microbial Cell Factories*. *8*, 54. doi.org/10.1186/1475-2859-8-54.

Choe, K. I., Kwon, J. H., Park, K. H., Oh, M. H., Kim, M. H., Kim, H. H., Cho, S. H., Chung, E. K., Ha, S. Y., & Lee, M. W. (2012) The antioxidant and anti-inflammatory effects of phenolic compounds isolated from the root of *Rhodiola sachalinensis* A. BOR. *Molecules*. *17*, 11484-11494. doi.org/10.3390/molecules171011484.

Chung, D., Kim, S. Y., & Ahn, J. H. (2017) Production of three phenylethanoids, tyrosol, hydroxytyrosol, and salidroside, using plant genes expressing in *Escherichia coli*. *Scientific Reports*. *7*, 2578. doi.org/10.1038/s41598-017-02042-2.

Flamholz, A., Noor, E., Bar-Even, A., & Milo, R. (2012) eQuilibrator-the biochemical thermodynamics calculator. *Nucleic Acids Research*. *40*, D770-775. doi.org/10.1093/nar/gkr874.

Fu, J., Bian, X. Y., Hu, S. B, Wang, H. L., Huang, F., Seibert, P. M., Plaza, A., Xia, L. Q., Müller, R., Stewart, A. F., & Zhang, Y. M. (2012) Full-length RecE

enhances linear-linear homologous recombination and facilitates direct cloning for bioprospecting. *Nature Biotechnology*. *30*, 440-446. doi.org/10.1038/nbt.2183.

Gold, N. D., Gowen, C. M., Lussier, F. X., Cautha, S. C., Mahadevan, R., & Martin, V. J. (2015) Metabolic engineering of a tyrosine-overproducing yeast platform using targeted metabolomics. *Microbial Cell Factories*. *14*, 73. doi.org/10.1186/s12934-015-0252-2.

Goldstein, A. L., & McCusker, J. H. (1999) Three new dominant drug resistance cassettes for gene disruption in *Saccharomyces cerevisiae*. *Yeast*. *15*, 1541-1553. doi.org/10.1002/(SICI)1097-0061(199910)15:14<1541::AID-YEA476>3.0.CO;2-K.

Gottardi, M., Reifenrath, M., Boles, E., & Tripp, J. (2017) Pathway engineering for the production of heterologous aromatic chemicals and their derivatives in *Saccharomyces cerevisiae*: bioconversion from glucose. *FEMS Yeast Research*. *17*. doi.org/10.1093/femsyr/fox035.

Granados-Principal, S., Quiles, J. L., Ramirez-Tortosa, C. L., Sanchez-Rovira, P., & Ramirez-Tortosa, M. C. (2010) Hydroxytyrosol: from laboratory investigations to future clinical trials. *Nutrition Reviews*. *68*, 191-206. doi.org/10.1111/j.1753-4887.2010.00278.x.

Grüning, N. M., Rinnerthaler, M., Bluemlein, K., Mülleder, M., Wamelink, M. M., Lehrach, H., Jakobs, C., Breitenbach, M., & Ralser, M. (2011) Pyruvate kinase triggers a metabolic feedback loop that controls redox metabolism in respiring cells. *Cell Metabolism*. *14*, 415-427. doi.org/10.1016/j.cmet.2011.06.017.

Gueldener, U., Heinisch, J., Koehler, G. J., Voss, D., & Hegemann, J. H. (2002) A

second set of loxP marker cassettes for Cre-mediated multiple gene knockouts in budding yeast. *Nucleic Acids Research*. *30*, e23. doi.org/10.1093/nar/30.6.e23.

Guo, W., Huang, Q. L., Liu, H., Hou, S. L., Niu, S. H., Jiang, Y., Bao, X. M., Shen, Y., & Fang, X. (2019) Rational engineering of chorismate-related pathways in *Saccharomyces cerevisiae* for improving tyrosol production. *Frontiers in Bioengineering and Biotechnology*. *7*, 152. doi.org/10.3389/fbioe.2019.00152

Hassing, E. J., de Groot, P. A., Marquenie, V. R., Pronk, J. T., & Daran, J. G. (2019) Connecting central carbon and aromatic amino acid metabolisms to improve de novo 2-phenylethanol production in *Saccharomyces cerevisiae*. *Metabolic Engineering*. *56*, 165-180. doi.org/10.1016/j.ymben.2019.09.011.

Hazelwood, L. A., Daran, J. M., van Maris, A. J., Pronk, J. T., & Dickinson, J. R. (2008) The ehrlich pathway for fusel alcohol production: a century of research on *Saccharomyces cerevisiae* metabolism. *Applied and Environmental Microbiology*. *74*, 2259-2266. doi.org/10.1128/AEM.02625-07.

Jiang, J. J., Yin, H., Wang, S., Zhuang, Y. B., Liu, S. W., Liu, T., & Ma, Y. H. (2018) Metabolic engineering of *Saccharomyces cerevisiae* for high-Level production of salidroside from glucose. *Journal of Agricultural and Food Chemistry*. *66*, 4431-4438. doi.org/10.1021/acs.jafc.8b01272.

Jiang, Y., Shen, Y., Gu, L, Wang, Z., Su, N., Niu, K., Guo, W., Hou, S., Bao, X., Tian, C, & Fang, X. (2020) Identification and characterization of an efficient d-xylose transporter in *Saccharomyces cerevisiae*. *Journal of Agricultural and Food Chemistry*. *68*, 2702-2710. doi.org/10.1021/acs.jafc.9b07113.

Kallscheuer, N., Menezes, R., Foito, A., Silva, M., Braga, A., Dekker, W.,

Sevillano, D. M., Rosado-Ramos, R., Jardim, C., Oliveira, J., Ferreira, P., Rocha, I., Silva, A. R., Sousa, M., Allwood, J., Bott, M., Faria, N., Stewart, D., Ottens, M., Naesby, M., Santos,C., & Marienhagen, J. (2019) Identification and microbial production of the *raspberry* phenol salidroside that is active against Huntington's disease. *Plant Physiology. 179*, 969–985. doi.org/10.1104/pp.18.01.

Lee, J. H., & Wendisch, V. F. (2017) Biotechnological production of aromatic compounds of the extended shikimate pathway from renewable biomass. *Journal of Biotechnology*. *257*, 211-221. doi.org/10.1016/j.jbiotec.2016.11.016.

Liu, Q. L., Yu, T., Li, X. W., Chen, Y., Campbell, K., Nielsen, J., & Chen, Y. (2019) Rewiring carbon metabolism in yeast for high level production of aromatic chemicals. *Nature Communications*. *10*, 4976. doi.org/10.1038/s41467-019-12961-5.

Meadows, A. L., Hawkins, K. M., Tsegaye, Y., Antipov, E., Kim, Y., Raetz, L., Dahl, R. H., Tai, A., Mahatdejkul-Meadows, T., Xu, L., Zhao, L., Dasika, M. S., Murarka, A., Lenihan, J., Eng, D., Leng, J. S., Liu, C. L., Wenger, J. W., Jiang, H., Chao, L., Westfall, P., Lai, J., Ganesan, S., Jackson, P., Mans, R., Platt, D., Reeves, C. D., Saija, P. R., Wichmann, G., Holmes, V. F., Benjamin, K., Hill, P. W., Gardner, T. S., & Tsong, A. E. (2016) Rewriting yeast central carbon metabolism for industrial isoprenoid production. *Nature*. *537*, 694-697. doi.org/10.1038/nature19769.

Minard, K. I., & McAlister-Henn, L. (2005) Sources of NADPH in yeast vary with carbon source. *The Journal of Biological Chemistry*. *280*, 39890-39896. doi.org/10.1074/jbc.M509461200

Nielsen, J. (2019) Yeast systems biology: model organism and cell factory. *Biotechnology Journal*. 14. doi.org/10.1002/biot.201800421.

Nocon, J., Steiger, M., Mairinger, T., Hohlweg, J., Rußmayer, H., Hann, S., Gasser, B., & Mattanovich, D. (2016) Increasing pentose phosphate pathway flux enhances recombinant protein production in *Pichia pastoris*. *Applied Microbiology and Biotechnology*. *100*, 5955–5963. doi.org/10.1007/s00253-016-7363-5.

Plomer, J. J., & Gafni, A. (1992) Denaturation of glucose-6-phosphate dehydrogenase from *Leuconostoc mesenteroides* by guanidine hydrochloride; identification of inactive, partially unfolded, dimeric intermediates. *Biochimica et Biophysica Acta*. *1122*, 234-242. doi.org/10.1016/0167-4838(92)90398-W.

Sadowski, I., Lourenco, P., & Parent, J. (2008) Dominant marker vectors for selecting yeast mating products. *Yeast*. *25*, 595-599. doi. org/10.1002/yea.1604.

Satoh, Y., Tajima, K., Munekata, M., Keasling J. D., & Lee, T. S. (2012) Engineering of a tyrosol-producing pathway, utilizing simple sugar and the central metabolic tyrosine, in *Escherichia coli*. *Journal of Agricultural and Food Chemistry*. *60*, 979-984. doi.org/10.1021/jf203256f.

Seike, T., Kobayashi, Y., Sahara, T., Ohgiya, S., Kamagata, Y., & Fujimori, K. E. (2019) Molecular evolutionary engineering of xylose isomerase to improve its catalytic activity and performance of micro-aerobic glucose/xylose co-fermentation in *Saccharomyces cerevisiae*. *Biotechnology for Biofuels*. *12*, 139. doi.org/10.1186/s13068-019-1474-z.

Soejima, H., Tsuge, K., Yoshimura, T., Koganemaru, K., & Kitagaki, H. (2012) Breeding of a high tyrosol-producing sake yeast by isolation of an ethanol-resistant mutant form *trp3* mutant. *Journal of The Institute of Brewing*. *118*, 264–268. doi.org/10.1002/jib.46.

Suástegui, M., Guo, W. H., Feng, X. Y., & Shao, Z. Y. (2016) Investigating strain dependency in the production of aromatic compounds in *Saccharomyces cerevisiae*. *Biotechnology and Bioengineering*. *113*, 2676-2685. doi.org/10.1002/bit.26037.

Torrens-Spence, M. P., Pluskal, T., Li, F. S., Carballo, V., & Weng, J. K. (2018) Complete pathway elucidation and heterologous reconstitution of *Rhodiola* Salidroside biosynthesis. *Molecular Plant. 11*, 205-217. doi.org/10.1016/j.molp.2017.12.007.

Wang, D. P., Wang, L., Hou, L., Deng, X. H., Gao, Q., & Gao, N. F. (2015) Metabolic engineering of *Saccharomyces cerevisiae* for accumulating pyruvic acid. *Annals of Microbiology. 65*, 2323-2331. doi.org/10.1007/s13213-015-1074-5.

Wang, F. Z., Jiang, Y., Guo, W., Niu, K. L., Zhang, R. Q., Hou, S. L., Wang, M. Y., Yi, Y., Zhu, C. X., Jia, C. J. & Fang, X. (2016). An environmentally friendly and productive process for bioethanol production from potato waste. *Biotechnology for Biofuels*. *9*, 50. doi.10.1186/s13068-016-0464-7.

Xue, Y. X., Chen, X. Z., Yang, C., Chang, J. Z., Shen, W., & Fan, Y. (2017) Engineering *Eschericha coli* for enhanced tyrosol production. *Journal of Agricultural and Food Chemistry*. *65*, 4708-4714.

doi.org/10.1021/acs.jafc.7b01369.

Yang, C., Chen, X. Z., Chang, J. Z.,Zhang, L. H., Xu, W., Shen, W., & Fan, Y. (2018) Reconstruction of tyrosol synthetic pathways in *Escherichia coli*. *Chinese Journal of Chemical Engineering*. *26*, 2615-2621. doi.org/10.1016/j.cjche.2018.04.020.

Zhu, L. P., Wei, T. T., Gao, J., Chang, X. Y., He, H., Luo, F., Zhou, R., Ma, C. H., Liu, Y., & Yan, T. H. (2015) The cardioprotective effect of salidroside against myocardial ischemia reperfusion injury in rats by inhibiting apoptosis and inflammation. *Apoptosis*. *20*, 1433-1443. doi.org/10.1007/s10495-015-1174-5.

Tables

Table 1 Comparison of thermodynamic data for the Xfpk-based pathway and the pentose phosphate pathway for E4P synthesis

Pathway thermodynamics	**The Xfpk-based pathway**	**The pentose phosphate pathway**
$\Delta_r G'^{m}$ (kJ/mol)	-129.2	-102.7
MDF (kJ/mol)	20.3	10.3
Steps	3	8
Coenzymes	0	4

Maximum theoretical performance	C-mol yield (C-mol/C-mol)	66.67%	33.33%
	Molar yield (mol/mol)	100%	50%

The thermodynamic analysis of the Xfpk-based pathway and the pentose phosphate pathway was carried out in the website of eQuilibrator (http://equilibrator.weizmann.ac.il). $\Delta_r G'^m$: the reaction Gibbs energy. Steps: the sum of the reactions from $_D$-glucose to $_D$-erythrose 4-phosphate in the studied pathway. MDF: the max-man driving force. Coenzymes: the sum of the coenzymes needed in the studied pathway converting 2 $_D$-glucose molecules into $_D$-erythrose 4-phosphate. C-mol yield (C-mol/C-mol) is the moles of carbon in $_D$-erythrose 4-phosphate from moles of carbon in $_D$-glucose. Molar yield (mol/mol) is the moles of $_D$-erythrose 4-phosphate per moles of glucose.

Table 2 Summary of recent reports regarding the production of tyrosol and salidroside from glucose

Products	**Organisms**	**Titer (g/L)**	**Productivity (mg/L/h)**	**Culture style**	**References**
Tyrosol	*E. coli*	0.069	1.44	Shake flask cultivation	Satoh et al. (2012)

Tyrosol	*E. coli*	0.573	11.94	Shake flask cultivation	Xue et al. (2017)
Tyrosol	*E. coli*	1.32	27.5	Shake flask cultivation	Yang et al. (2018)
Salidroside	*E. coli*	0.057	1.19	Shake flask cultivation	Bai et al. (2014)
Salidroside/Tyrosol	*E. coli*	0.531 (Tyrosol) 0.288(Salidroside)	22.13 (Tyrosol) 12 (Salidroside)	Shake flask cultivation	Chung et al. (2017)
Tyrosol	*S. cerevisiae*	0.115	2.39	Shake flask cultivation	Guo et al. (2019)
Salidroside	*S. cerevisiae*	0.0015	0.03	Shake flask cultivation	Torrens-Spence et al. (2018)
Salidroside/Tyros	*S. cerevisiae*	1.395 (Tyrosol) 0.733	11.63 (Tyrosol) 6.11	Fed-batch fermentation	Jiang et al. (2018)

ol		(Salidrosid e)	(Salidrosid e)		
Salidroside	*Corynebacterium glutamicum*	0.64 (Salidrosid e)	8.88 (Salidrosid e)	Shake flask cultivation	Kallscheuer et al. (2019)
Products	**Organisms**	**Titer (g/L)**	**Productivity (mg/L/h)**	**Culture style**	**References**
Salidroside/ Tyrosol	*S. cerevisiae*	8.48 (Tyrosol) 1.82 (Salidrosid e)	49.70 (Tyrosol) 9.87 (Salidrosid e)	Fed-batch fermentation	This work

Table 3 Strains used in this study

Strains	**Description**	**Genotype**	**Sources**
HLF-	WT	*MATα, HO::loxp*	Present

Dα			work
DA-0	*PDC1::EcTyrA*$^{M53I/A354V}$	HLF-DA; *PDC1::EcTyrA*$^{M53I/A354V}$-*T*$_{CYC1}$-*loxp*	Present work
DA-1	*PDC1::EcTyrA*$^{M53I/A354V}$; *YJRWdelta12::PcAAS*^{syn}	DA-0; *YJRWdelta12::P*$_{TDH3}$-*PcAAS*^{syn}-*T*$_{CYC1}$-*natMX4*	Present work
DA-2	*PDC1::EcTyrA*$^{M53I/A354V}$; *YJRWdelta12::PcAAS*^{syn}; *PHA2*Δ	DA-1; *PHA2::loxp-kanMX4-loxp*	Present work
DA-3	*PDC1::EcTyrA*$^{M53I/A354V}$; *YJRWdelta12::PcAAS*^{syn}; *PHA2::ZWF1*	DA-1; *PHA2::P*$_{TPI1}$-*ZWF1-T*$_{GPM1}$-*loxp-kanMX4-loxp*	Present work
DA-4	*PDC1::EcTyrA*$^{M53I/A354V}$; *YJRWdelta12::PcAAS*^{syn}; *PHA2::Baxfpk*	DA-1; *PHA2::P*$_{TPI1}$-*Baxfpk-T*$_{GPM1}$-*loxp-kanMX4-loxp*	Present work
DA-5	*PDC1::EcTyrA*$^{M53I/A354V}$; *YJRWdelta12::PcAAS*^{syn}; *GRE3*Δ	DA-1; *GRE3::loxp-kanMX4-loxp*	Present work

Strains	Description	Genotype	Sources
DA-6	*PDC1::EcTyrA*$^{M53I/A354V}$; *YJRWdelta12::PcAAS*^{syn}; *GRE3::Baxfpk*	DA-1; *GRE3::*P_{TPI1}*-Baxfpk-*T_{GPM1}*-loxp-kanMX4-loxp*	Present work
DA-7	*PDC1::EcTyrA*$^{M53I/A354V}$; *YJRWdelta12::PcAAS*^{syn}; *XKS1*Δ	DA-1; *XKS1::loxp-kanMX4-loxp*	Present work
DA-8	*PDC1::EcTyrA*$^{M53I/A354V}$; *YJRWdelta12::PcAAS*^{syn}; *XKS1::Baxfpk*	DA-1; *XKS1::*P_{TPI1}*-Baxfpk-*T_{GPM1}*-loxp-kanMX4-loxp*	Present work
DA-9	*PDC1::EcTyrA*$^{M53I/A354V}$; *YJRWdelta12::PcAAS*^{syn}; *PHA2::Bbxfpk*	DA-1; *PHA2::*P_{TPI1}*-Bbxfpk-*T_{GPM1}*-loxp-kanMX4-loxp*	Present work
DA-10	*PDC1::EcTyrA*$^{M53I/A354V}$; *YJRWdelta12::PcAAS*^{syn}; *PHA2::Bdxfpk*	DA-1; *PHA2::*P_{TPI1}*-Bdxfpk-*T_{GPM1}*-loxp-kanMX4-loxp*	Present work
DA-41	*PDC1::EcTyrA*$^{M53I/A354V}$;	DA-4; *GPP1::loxp-kanMX4-*	Present

	YJRWdelta12::PcAAS^{syn}; *PHA2::Baxfpk*; *GPP1*Δ	*loxp*	work

Strains	**Description**	**Genotype**	**Sources**
DA-42	*PDC1::EcTyrA*$^{M53I/A354V}$; *YJRWdelta12::PcAAS*^{syn}; *PHA2::Baxfpk*; *GPP1::Ckpta*	DA-4; *GPP1::*P_{TDH3}*-Ckpta-*T_{PGK1}*-loxp-kanMX4-loxp*	Present work
DA-9-1	*PDC1::EcTyrA*$^{M53I/A354V}$; *YJRWdelta12::PcAAS*^{syn}; *PHA2::Bbxfpk*; *TRP3*Δ	DA-9; *TRP3::hphMX4*	Present work
DA-91	*PDC1::EcTyrA*$^{M53I/A354V}$; *YJRWdelta12::PcAAS*^{syn}; *PHA2::Bbxfpk*; *TRP3::ugt85a1*	DA-9; *TRP3::*P_{TEF1}*-ugt85a1-*T_{CYC1}*-hphMX4*	Present work

Figures

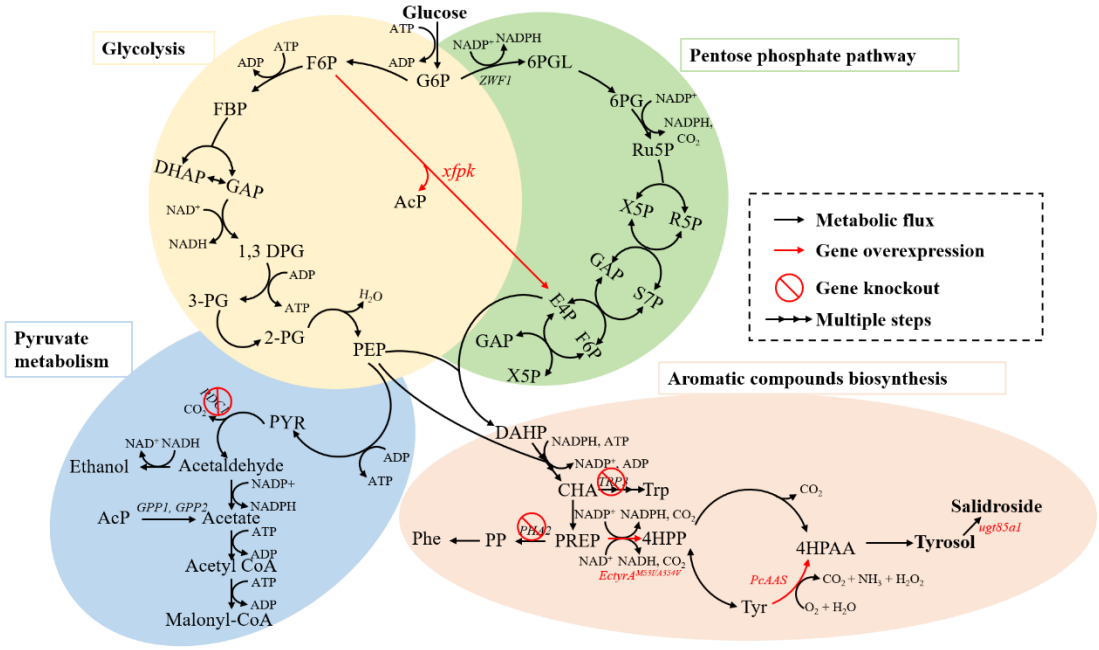

Fig. 1 Engineering of the biosynthesis pathway from glucose to tyrosol in *S. cerevisiae* Compounds: G6P, glucose 6-phosphate; F6P, fructose 6-phosphate; FBP, fructose 1,6-bisphosphate; DHAP, dihydroxyacetone phosphate; GAP, D-glyceraldehyde 3-phosphate; 1,3 DPG, 3-phospho-D-glyceroyl-phosphate; 3-PG, 3-phospho-D-glycerate; 2-PG, 2-phospho-D-glycerate; PEP, phosphoenolpyruvate; PYR, pyruvate; 6PGL, 6-phospho D-glucono-1,5-lactone; 6PG, D-gluconate 6-phosphate; Ru5P, D-ribulose 5-phosphate; X5P, D-xylulose 5-phosphate; R5P, D-ribose 5-phosphate; S7P, D-sedoheptulose 7-phosphate; E4P, D-erythrose 4-phosphate; AcP: acetyl phosphate; DAHP, 3-deoxy-D-arabino-heptulosonate 7-phosphate; CHA, chorismate; Trp, L-tryptophan; PREP, prephenate; PP, 3-phenyl-2-oxopropanoate; Phe, L-phenylalanine; 4HPP, 3-(4-hydroxyphenyl)pyruvate; Tyr, L-tyrosine; 4HPAA, 4-hydroxyphenylacetaldehyde.

Genes: *PDC1*, pyruvate decarboxylase 1 gene; *ZWF1*, glucose-6-phosphate dehydrogenase gene; *xfpk*, phosphoketolase gene; *PHA2*, prephenate dehydratase gene; *EctyrA*, chorismate mutase/prephenate dehydrogenase gene from *E. coli*; *PcAAS*, aromatic aldehyde synthase gene from *Petroselinum crispum*; *TRP3*, anthranilate synthase gene; *ugt85a1*, UDP-glycosyltransferase from *Arabidopsis thaliana*

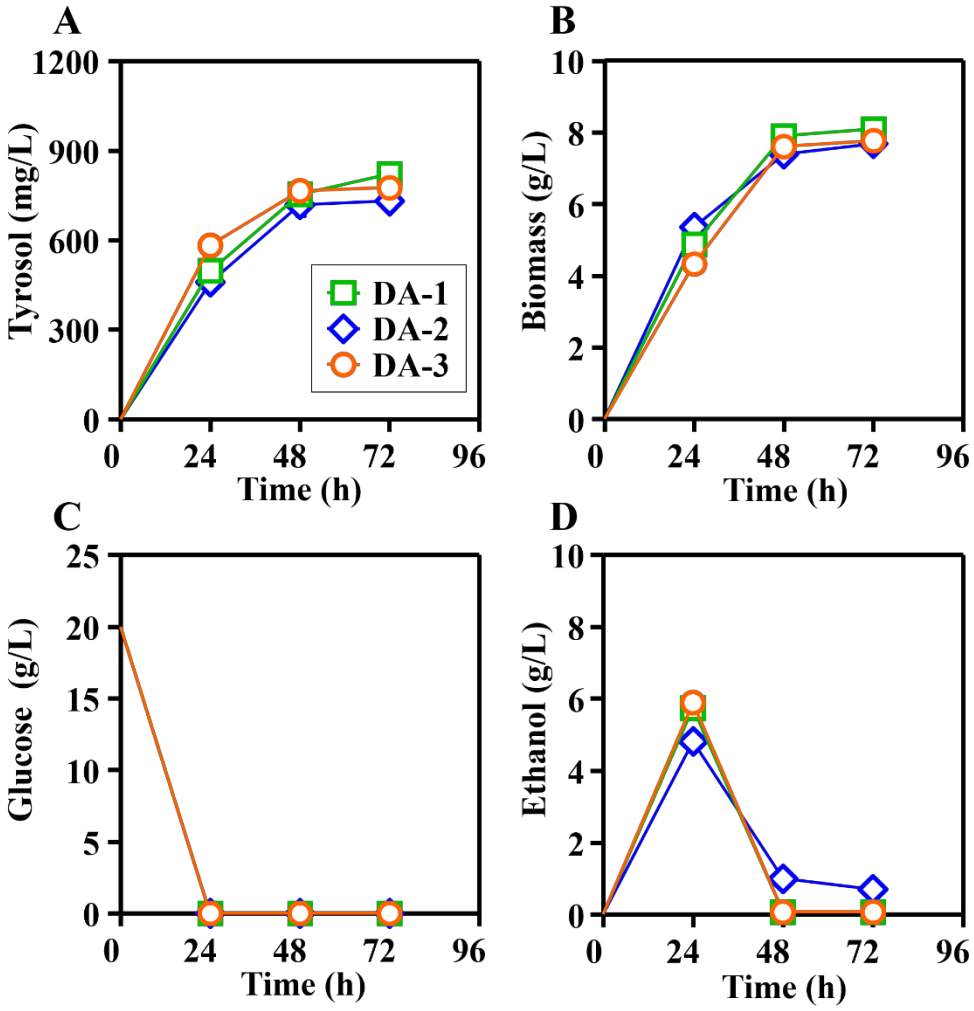

Fig. 2 Effects of overexpressing *ZWF1* on *S. cerevisiae*

Formation of tyrosol, glucose, and ethanol consumption and growth of strain DA-1 (*PDC1::EcTyrA*$^{M53I/A354V}$; *YJRWdelta12::PcAAS*^{syn}) and its derived strain

DA-2 (DA-1, *PHA2*Δ), DA-3 (DA-1, *PHA2::ZWF1*). (A) Tyrosol (mg/L); (B) Biomass (g/L); (C) Glucose (mg/L) and (D) Ethanol (g/L).

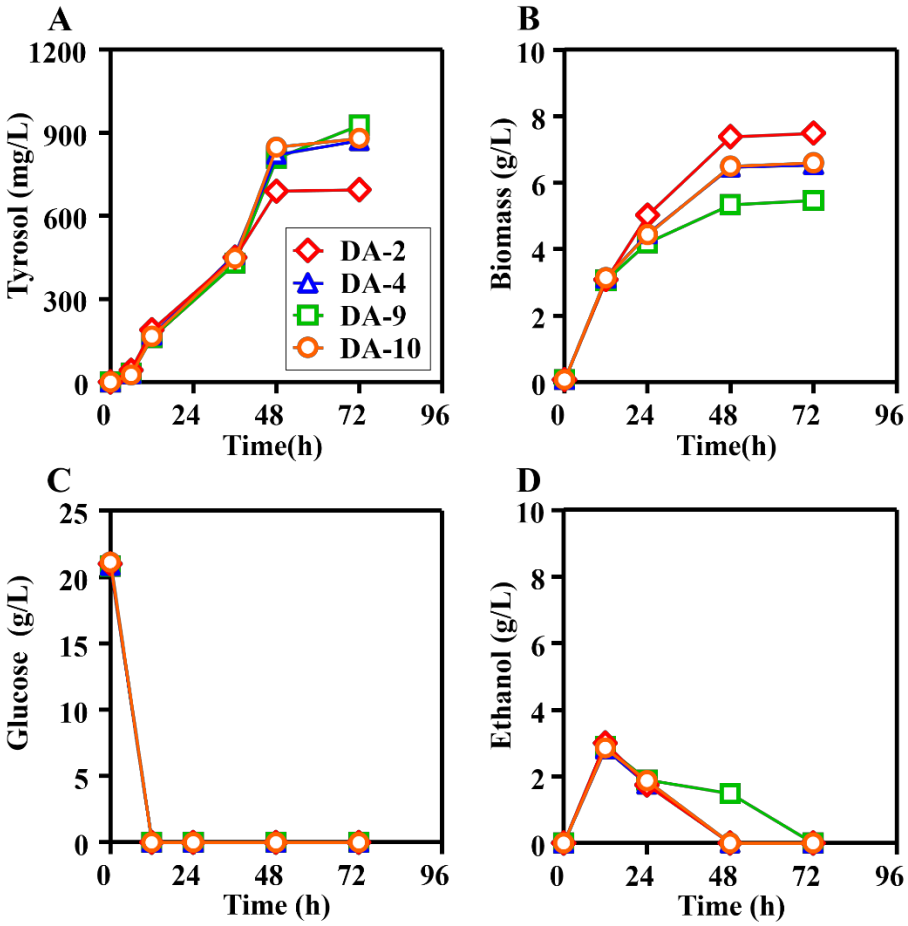

Fig. 3 Effects of the introduction of various phosphoketolases into *S. cerevisiae*

The formation of tyrosol and glucose, ethanol consumption and growth of DA-1 (*PDC1::EcTyrA*$^{M53I/A354V}$; *YJRWdelta12::PcAAS*^{syn}) derived strains DA-2 (DA-1, *PHA2*Δ), DA-4 (DA-1, *PHA2*::*Baxfpk*), DA-9 (DA-1, *PHA2*::*Bbxfpk*), and DA-10 (DA-1, *PHA2*::*Bdxfpk*) are shown. (A) Tyrosol (mg/L); (B) Biomass (g/L); (C) Glucose (mg/L) and (D) Ethanol (g/L).

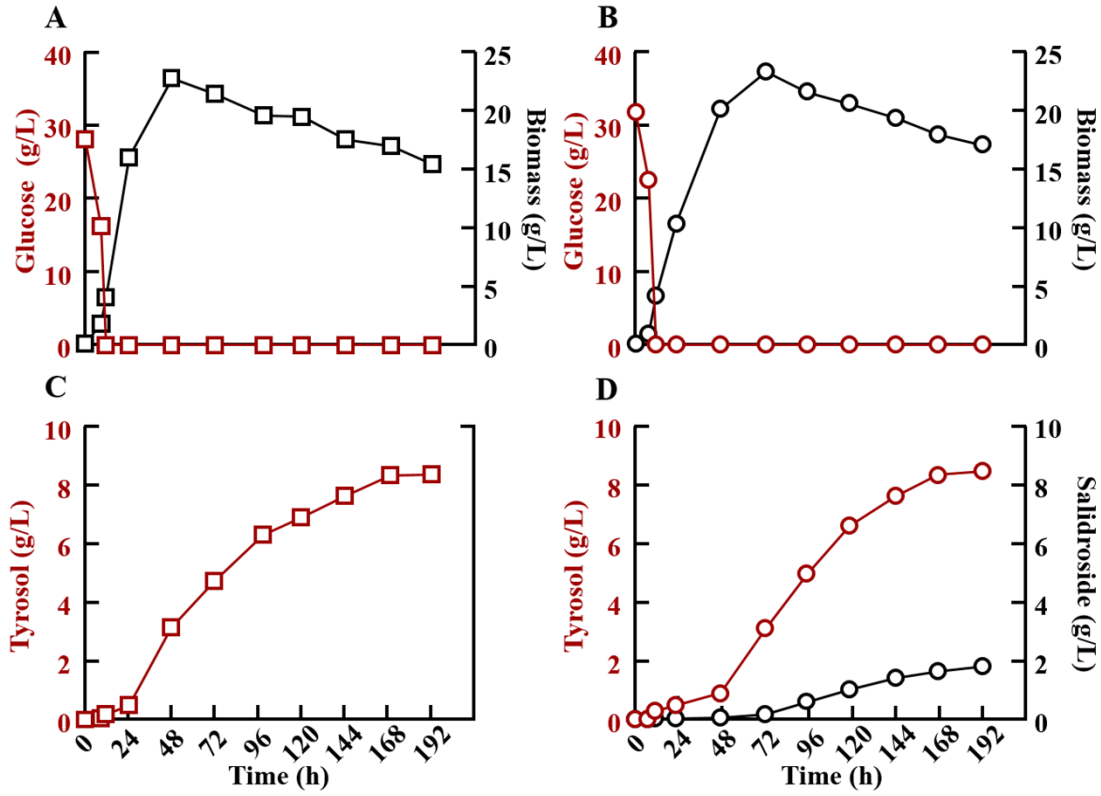

Fig. 4 Fed-batch fermentation performed using strains DA-9 and DA-91

Fermentation profiles of the best tyrosol-producing strain DA-9 (*PDC1::EcTyrA*$^{M53I/A354V}$, *YJRWdelta12::PcAAS*^{syn}, *PHA2::Bbxfpk*) and the salidroside-producing strain DA-91 (*PDC1::EcTyrA*$^{M53I/A354V}$, *YJRWdelta12::PcAAS*^{syn}, *PHA2::Bbxfpk, TRP3::ugt85a1*) during fed-batch fermentation for 192 h. (A) (B) Glucose (g/L) and biomass (g/L); (C) (D) Tyrosol concentration (g/L) and salidroside concentration (g/L).